ChemComm

Accepted Manuscript

ROYAL SOCIETY OF CHEMISTRY

rsc.li/chemcomm

View Article Online
DOI: 10.1039/C7CC02212C

Journal Name

COMMUNICATION

Bioorthogonal Double-Fluorogenic Siliconrhodamine Probes for Intracellular Super-resolution Microscopy‡

Received 00th January 20xx,
Accepted 00th January 20xx

DOI: 10.1039/x0xx00000x

www.rsc.org/

E. Kozma,[a] G. Estrada Girona,[b] G. Paci,[b] E. A. Lemke[b] and P. Kele*[a]

A series of double-fluorogenic siliconrhodamine probes was synthesized. These tetrazine-functionalized, membrane-permeable labels allowed site-specific bioorthogonal tagging of genetically manipulated intracellular proteins and subsequent imaging using super-resolution microscopy.

Recent years have brought substantial progress in the field of super-resolution microscopy (SRM) enabling the exploration of biomolecular processes in the sub-diffraction range.[1] Although the emerged SRM techniques have revealed fine details of live organisms, there is still room for further improvements. Nowadays, the unavailability of dyes suitable for site-specific tagging of intracellular biomolecules is considered as the biggest limitation of SRM techniques.[2] Ideal small-sized organic fluorophores can be synthetically tailored in order to meet the criteria necessary for intracellular SRM imaging of live cells. Such criteria are: (a) both the labels themselves and the chemistry applied for tagging should be biocompatible, (b) their photophysical characteristics should allow minimal background and autofluorescence in order to result in high signal-to-noise (S/N) ratio, (c) their fluorescence should be bright and not or minimally impaired by photobleaching and (d) they should be able to transit through membranes. As of the chemistry applied for installation of such probes, bioorthogonal reactions are extremely useful as they are fully biocompatible.[3] Among these transformations, inverse electron demand Diels-Alder (IEDDA) reactions between tetrazines and strained unsaturated ring systems enable the fastest reactions.[4] In order to minimize phototoxicity and autofluorescence, far-red/near-infrared (NIR) emitting fluorophores (650-900 nm) are especially well suited, while background fluorescence of unreacted probes bound non-specifically to hydrophobic surfaces can be reduced efficiently by the use of fluorogenic species.[5,6]

Our continuing efforts to develop fluorescent probes that combine the above listed features have resulted in several bioorthogonally applicable fluorogenic probes with various excitation/emission characteristics.[7] Lately, our attention turned to tetrazine quenched fluorescent frameworks as tetrazines can act both as bioorthogonal handles and quencher moieties.[7d] Tetrazines can exert their quenching effect either by Förster-resonance energy transfer (FRET) or through-bond energy transfer (TBET) mechanisms.[8,9] FRET-based fluorogenic probes are limited to tetrazine-fluorophore pairs where the absorption band of the tetrazine (typically between 520-540 nm) overlaps with the emission band of the fluorophore. TBET based systems, on the other hand, are not constrained by the emission band of the fluorescent unit and, in theory, any kind of fluorophore-tetrazine pairs are suitable upon proper design. Moreover, TBET-based quenching is much faster and more efficient, thus enhancement of the fluorescence signal can reach up to 11,000-fold upon IEDDA reaction with dienophiles.[9a] The tetrazine-based TBET-quenching approach has already been applied to various fluorophores, yet, it has not been performed on SRM compatible dyes.[9] However, techniques like SRM would greatly benefit from the high signal-to-noise ratio offered by TBET-mechanism.

Siliconrhodamine (SiR) is a widely used membrane-permeable NIR dye for SRM applications.[10] Besides the high photostability and brightness, the unique environment-dependent fluorescence of carboxy-SiRs due to a polarity dependent lactone-formation offers an appealing opportunity to distinguish between specific and non-specific labeling, (polarity-based fluorogenicity).[10] When bound to polar protein surfaces, carboxyl-SiRs exist in a fluorescent zwitterionic form, while upon non-specific adhesion to hydrophobic surfaces, it closes to non-fluorescent spirolactone (Figure 1). SiR derivatives were applied in voltage sensing, *in vivo* tumor imaging, photodynamic therapy and multicolour imaging studies as well.[11] Despite their wide applications, there are only a few examples of SiR-based probes for site-specific labeling of proteins.[10a,12,13] Furthermore, no TBET-based carboxyl-SiR fluorogenic probes were reported yet.

Herein we report the first set of bioorthogonally applicable, NIR-emitting, membrane permeable, double fluorogenic

[a] "Lendület" Chemical Biology Research Group, Institute of Organic Chemistry, Research Centre for Natural Sciences, Hungarian Academy of Sciences, Magyar tudósok krt. 2, 1117 Budapest, Hungary. E-mail: kele.peter@ttk.mta.hu
[b] Structural and Computational Biology Unit, Cell Biology and Biophysics Unit European Molecular Biology Laboratory D-69117, Heidelberg, Meyerhofstrasse 1.,Germany

Electronic Supplementary Information (ESI) available: [details of any supplementary information available should be included here]. See DOI: 10.1039/x0xx00000x

View Article Online
DOI: 10.1039/C7CC02212C

probes suitable for SRM imaging with exceptionally high turn-on rates compared to previously reported tetrazine-based NIR dyes.[9d] We demonstrate the power of the developed SiR-dyes in site-specific labeling of intracellular skeletal proteins and subsequent SRM imaging applications.

TBET-based fluorogenic probes are composed of a donor fluorophore and an acceptor tetrazine unit that are linked together with a conjugated but electronically decoupled (twisted) linker.[14] The tetrazine moiety can be installed onto the phenyl group of SiR directly or via alkene, alkyl and phenyl linkers. Former examples showed that incorporation of the tetrazine through direct conjugation or via alkyl-linkers to fluorophores is less efficient.[9c,d,f] Therefore we decided to apply alkene and phenyl linkers to connect the tetrazine to carboxy-SiR. Devaraj and co-workers and also our group have recently reported Heck- and Suzuki-type cross-coupling reactions to connect methyl-substituted tetrazines to fluorophores.[7d,9b] To this end we have synthesized Br-substituted intermediate **6**. The general synthetic route for SiR derivatives proceeds through a Si-xantone intermediate which is reacted with aryl lithium reagents via nucleophilic addition.[10a] Through this route, however, introduction of halogen-substituted aromatic rings is problematic. Therefore we proceeded via an aldehyde condensation reaction developed by Wang *et al*. (Scheme 1) and acquired Br-SiR derivative **6**.[15a]

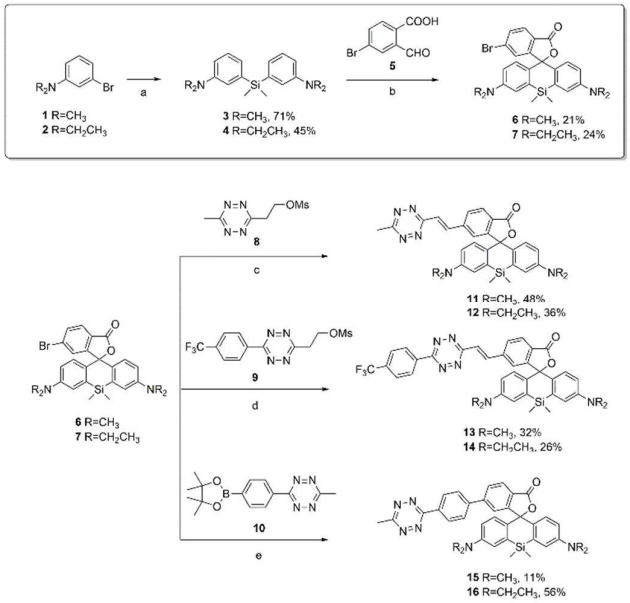

Scheme 1. Synthesis of SiR dyes **11**-**16**. Reaction conditions: a) *i*) *n*-BuLi, THF, -78 °C, 2 h; *ii*) $SiCl_2Me_2$, rt, 16 h; b) $CuBr_2$, 140 °C, 16 h; c) $Pd_2(dba)_3$, QPhos, $(Cy)_2NMe$, DMF, 50 °C, 40 min, MW; d) $Pd_2(dba)_3$, QPhos, DIPEA, 1,4-dioxane, 90-110 °C, 16 h; e) $PdCl_2(dppf)$, Cs_2CO_3, 1,4-dioxane, 90 °C, 16 h.

We positioned the Br-substituent at the 6-position as previous reports showed superior fluorogenic properties of 6-substituted rhodamine derivatives compared to 5-substitution.[9d,f] Pd-catalyzed cross-coupling reactions of **6** with methyl vinyltetrazine precursor (**8**) and methyltetrazine phenylboronic acid pinacol ester (**10**) resulted in alkene- (**11**) and phenyl-linked SiR-tetrazine (**15**), respectively, with moderate to good yields (11-48%). To improve reaction rate of alkene-linked SiR-tetrazine in IEDDA, we designed a derivative with trifluoromethyl-phenyl substituent. Electron-withdrawing groups are known to markedly increase the reactivities of tetrazines in IEDDA reactions.[4a] To this end, we synthesized trifluormethyl-tetrazine (**9**) in two steps via $Zn(OTf)_2$ catalyzed Pinner-synthesis and subsequent O-mesylation.[15b] Heck-reaction of tetrazine **9** with compound **6** proceeded with moderate yields (32%). It is known that different N-alkylation patterns on the rhodamine core can markedly alter spectral characteristics and brightness of probes.[16] Rotation about the C-N bond in $-NMe_2$ substituted rhodamines leads to faster decay of the excited state thus lowered quantum yield. Thus we synthesized $-NEt_2$ substituted derivatives (**12**, **14**, **16**) starting from Br-SiR derivative **7**, which have restricted C-N bond rotation compared to $-NMe_2$ derivatives.

Next, we characterized the spectral properties of SiR-tetrazines **11**-**16**. Measurements were conducted in water containing 0.01% SDS to prevent aggregation of the dyes.[10a] Excitation maxima were found to be at around 645 nm and 655 nm, and fluorescence emission was detected at around 665 nm and 670 nm for the dimethylamino- and diethylamino-derivatives, respectively (Figure S1, see ESI). We measured the fluorogenic properties of the probes in an IEDDA reaction with OxTCO (**17**) (Figure 1, S2, Table 1).[7d] To our delight, all derivatives showed much larger fluorescence enhancements (FE) than formerly reported fluorogenic tetrazine NIR dyes (*cf*. 5.6x).[9d] We propose that this is attributed to the double fluorogenic nature of our SiR dyes. Among dimethylamine derivatives, phenyl-linked **15** showed the highest turn-on ratio (31x). As expected, ethyl substitution on the N-atom improved turn-on rates of the dyes, and up to 49-fold increase was observed. Although energy transfer occurs from the excited state, interestingly, the extinction coefficients were measured to be lower than ε of parent fluorophores (Table 1).

Table 1. Photophysical properties of SiR dyes **11**-**16**.

Dye	$\lambda_{exc(max)}$ [nm][a]	$\lambda_{em(max)}$ [nm][a]	ε_{max} [$M^{-1}cm^{-1}$][a,b]	ϕ_F[a,c]	$\Delta\phi_F$[d]	FE[e]
11	643 (645)	665 (667)	19,700 (19,200)	0.016 (0.34)	21	22
12	653 (652)	671 (672)	20,600 (19,800)	0.015 (0.80)	50	49
13	647 (648)	662 (665)	26,200 (22,500)	0.028 (0.26)	9	6
14	655 (654)	673 (672)	29,000 (25,600)	0.037 (0.27)	7	8
15	645 (644)	660 (660)	23,000 (21,600)	0.012 (0.34)	28	31
16	651 (652)	671 (670)	26,000 (23,900)	0.015 (0.53)	35	40

[a] values refer to tetrazine-dyes while values in parenthesis are that of the respective conjugates with **17**; [b] measured at absorption maxima of the species; [c] cresyl violet in MeOH was used as quantum yield reference (ϕ_F = 0.53); [d] quantum yield ratios of conjugates with **17** and tetrazine-dyes in 0.1% SDS in water; [e] fluorescence intensity enhancements upon reaction with **17** in 0.1% SDS in water at products emission maxima.

View Article Online
DOI: 10.1039/C7CC02212C

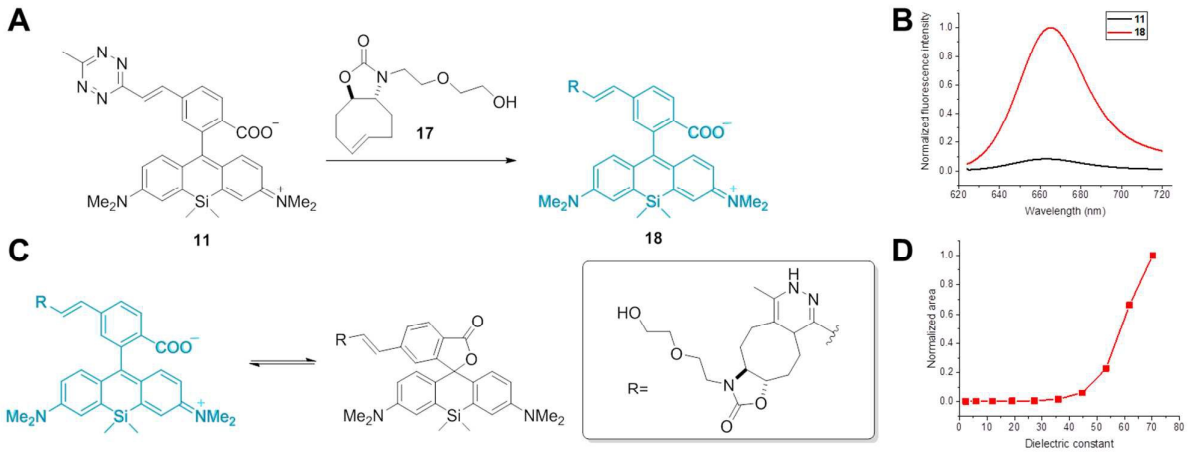

Figure 1. a) F*luorogenicity of SiR dyes*: IEDDA reaction between **11** and **17** resulting in fluorescence turn-on upon the formation of conjugate **18** due to the transformation of quenching tetrazine moiety into dihydropyridazine during reaction. b) Corresponding fluorescence emission spectra of free dye **11** (black) and conjugate **18** (red) showing fluorescence turn-on upon reaction. c) *Polarity-dependent fluorogenicity of SiR dyes*: conjugate **18** is present in fluorescent open, zwitterionic form in polar environment, and in non-fluorescent closed spirolactone form in apolar solvents. d) Normalized integral of fluorescence spectra of **18** in water-dioxane mixtures as a function of dielectric constant. Conjugate **18** is in fluorescent zwitterionic form in solvents with dielectric constant >50.

The second order rate constants were also determined and were in good agreement with k_2 values of previously reported methyl-tetrazine derivatives with similarly reactive TCO* (for values see ESI).[17] As expected, trifluoromethylphenyl derivatives, **13** and **14** reacted much faster than methyl derivatized congeners with OxTCO (**17**) (Figure S3). Due to the lower electron density of the tetrazines in **13** and **14** IEDDA reactions went to completion within minutes compared to methyl substituted probes where reaction required ca. 1.5 h.

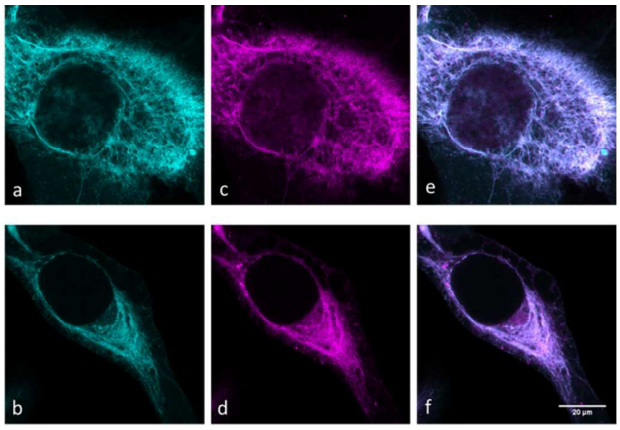

Figure 2. Confocal images of live cell SiR-labeling of vimentin^{BCNendo}–mOrange with dyes **11** (a,c,e) and **12** (b,d,f). Left to right: reference channel (mOrange-cyan) (a,b), labeling channel (c, d) and overlay (e,f). Labeling was performed at 3 µM for 10 min at 37 °C.

We also investigated the polarity dependent absorbance of the Diels-Alder product of alkene-SiR (**18**). In agreement with previous findings, in solvents with lower dielectric constants, absorption maximum, characteristic of the spirolactone form at 290 nm was dominant. In polar solvents, however, the zwitterionic form with a characteristic absorption at 645 nm dominated the spectrum (Figure S4). As a consequence, in solvents with dielectric constants <50 conjugate **18** was non-fluorescent while fluorescence gradually reinstated with increasing polarity (Figure 1).

With the SiR-dyes in hand, showing exceptional fluorogenicity in the NIR region, we were eager to evaluate their performance in the cellular environment. We sought to utilize genetic code expansion (GCE) technology for site-specific labeling with the newly developed double-fluorogenic probes. We and others have recently shown that non-canonical amino acids (ncAA) with strained alkene and alkyne moieties can be genetically encoded in mammalian cells using the pyrrolysine tRNA^{Pyl}/PylRS pair from *Methanosarcina* species.[18] We used the previously reported skeletal protein vimentin^{116TAG}-mOrange to test the intracellular labeling ability of the dyes.[13,18e] Using orthogonal tRNA^{Pyl}/PylRS^{AF} pair we genetically encoded commercially available cyclooctynylated-lysine (Lys(*ε*-*N*-BCN^{endo}), Figure S5) into vimentin^{116TAG}-mOrange and performed live cell labeling experiments with dyes **11**-**16** in mammalian cells. Clear live cell labeling was observed with dye **11** and **12** in concentrations as low as 1.5 µM within 10 min at 37 °C (Figure 2, for additional images at different concentrations and labeling times see Figure S6, S7, and for a comparison of different post-labeling washing time see Figure S8). The labeling was specific with no strong background fluorescence (as quantified by channel colocalisation in Figure S9). Less efficient labeling was observed with phenyl-linked dyes **15** and **16**, which is probably due to their slower kinetics (Figure S10). Although CF_3-dyes **13** and **14** showed the fastest labeling properties *in vitro*, they did not give any specific labeling *in vivo* (results not shown). We attribute this to the low polarity of these dyes, which probably impairs their ability to cross cell-membrane or to label the protein specifically.

To date, there are only a few reports on bioorthogonally applicable, fluorogenic tetrazine-mediated intracellular labeling inside living cells and subsequent SRM.[13,18e,19] Among them, to the best of our knowledge, there are no reports of

View Article Online
DOI: 10.1039/C7CC02212C

site-specific labeling with TBET-based fluorogens. We set out to test the suitability of dyes **11** and **12** in SRM of vimentin. While GSDIM SRM with TIRF illumination was possible with vimentin^{BCNendo}-mOrange labeled with dye **11**, we did not get any specific SRM signal with diethyl-derivative **12** (Figure 3). SRM imaging with SiR-**11** (Figure 3E, F) clearly gives enhanced resolution compared to the reference channels (Figure 3A-D, and Figure S11).

In conclusion, we have developed double-fluorogenic siliconrhodamine-tetrazine probes with improved kinetics and enhanced fluorescence turn-on ratios in the NIR region upon inverse electron demand Diels-Alder reactions. We have demonstrated the effect of the linker and *N*-alkylation pattern of the SiR-tetrazine core on labeling efficiency by confocal microscopy. We successfully applied one derivative in site-specific super-resolution imaging of a cytoskeletal protein, vimentin. Such probes with distinct spectral characteristics would allow multicolor super-resolution imaging of various intracellular structures.

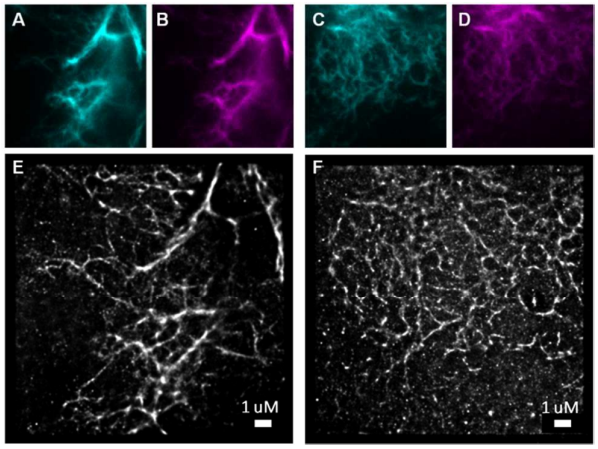

Figure 3. SRM imaging of vimentin^{BCNendo}-mOrange labeled with dye **11**. Panels A,C (cyan) and B,D (magenta) show the mOrange and SiR reference channels for the corresponding SRM images in panels E and F from dye **11** labeling (3 μM for 30 minutes at 37 °C). SRM images E and F have resolutions of 35 nm and 28 nm respectively as determined by the Fourier ring correlation criterion (FRC).[20]

Notes and references

‡ Present work was supported by the Hungarian Scientific Research Fund (OTKA, NN-116265) and the "Lendület" Program of the Hungarian Academy of Sciences (LP2013-55/2013). E.K. is grateful for the support of The New National Excellence Program of The Ministry of Human Capacities (Hungary). EAL acknowledges the SPP1623 and SFB1129 for funding.

1 a) M. Heilemann, *J. Biotechnol.*, 2010, **149**, 243; b) B. Huang, H. Babcock and X. Zhuang, *Cell*, 2010, **143**, 1047.
2 a) M. Fernández-Suárez and A. Y. Ting, *Nat. Rev. Mol. Cell Biol.*, 2008, **9**, 929; b) T. J. Chozinski, L. A. Gagnon and J. C. Vaughan, *FEBS Lett.*, 2014, **588**, 3603.
3 a) C. P. Ramil and Q. Lin, *Chem. Commun.*, 2013, **49**, 11007; b) J. A. Prescher and C. R. Bertozzi, *Nat. Chem. Biol.*, 2005, **1**, 13; c) E. M. Sletten and C. R. Bertozzi, *Angew. Chem. Int. Ed.*, 2009, **48**, 6974.
4 a) A.-C. Knall and C. Slugovc, *Chem. Soc. Rev.*, 2013, **42**, 5131; b) E. Kozma, O. Demeter and P. Kele, *ChemBioChem*, 2017, **18**, 486.
5 a) G. Cserép, A. Herner and P. Kele, *Methods Appl. Fluoresc.*, 2015, **3**, 042001; b) L. D. Lavis and R. T. Raines, *ACS Chem. Biol.*, 2014, **9**, 855.
6 A. Nadler and C. Schultz, *Angew. Chem. Int. Ed.*, 2013, **52**, 2408.
7 a) A. Herner, I. Nikić, M. Kállay, E. A. Lemke and P. Kele, *Org. Biomol. Chem.*, 2013, **11**, 3297; b) A. Herner, G. Estrada Girona, I. Nikić, M. Kállay, E. A. Lemke and P. Kele, *Bioconjugate Chem.*, 2014, **25**, 1370; c) O. Demeter, E. A. Fodor, M. Kállay, G. Mező, K. Németh, P. T. Szabó and P. Kele, *Chem. Eur. J.*, 2016, **22**, 6382; d) G. Knorr, E. Kozma, A. Herner, E. A. Lemke and P. Kele, *Chem. Eur. J.*, 2016, **22**, 8972.
8 a) N. K. Devaraj, S. Hilderbrand, R. Upadhyay, R. Mazitschek and R. Weissleder, *Angew. Chem. Int. Ed.*, 2010, **49**, 2869; b) J. Yang, J. Šečkutė, C. M. Cole and N. K. Devaraj, *Angew. Chem. Int. Ed.*, 2012, **51**, 7476.
9 a) L. G. Meimetis, J. C. T. Carlson, R. J. Giedt, R. H. Kohler and R. Weissleder, *Angew. Chem. Int. Ed.*, 2014, **53**, 7531; b) H. Wu, J. Yang, J. Šečkute and N. K. Devaraj, *Angew. Chem. Int. Ed.*, 2014, **53**, 5805 c) A. Wieczorek, T. Buckup and R. Wombacher, *Org. Biomol. Chem.*, 2014, **12**, 4177; d) A. Wieczorek, P. Werther, J. Euchner and R. Wombacher, *Chem. Sci.*, 2017, **8**, 1506; e) P. Agarwal, B. J. Beahm, P. Shieh and C. R. Bertozzi, *Angew. Chem. Int. Ed.*, 2015, **54**, 11504; f) J. C. T. Carlson *et al.*, *Angew. Chem. Int. Ed.*, 2013, **52**, 6917.
10 a) G. Lukinavičius *et al.*, *Nat. Chem.*, 2013, **5**, 132; b) S. Uno, *et al., Nat. Chem.*, 2014, **6**, 681; c) P. Shieh, M. S. Siegrist, A. J. Cullen and C. R. Bertozzi, *Proc. Natl. Acad. Sci. USA*, 2014, **111**, 5456.
11 Y. Kushida, T. Nagano and K. Hanaoka, *Analyst*, 2015, **140**, 685.
12 T. Peng and H. C. Hang, *J. Am. Chem. Soc.*, 2016, **138**, 14423.
13 C. Uttamapinant *et al.*, *J. Am. Chem. Soc.*, 2015, **137**, 4602.
14 a) T. G. Kim *et al., J. Phys. Chem. A*, 2006, **110**, 20; b) M. Steeger, S. Griesbeck, A. Schmiedel, M. Holzapfel, I. Krummenacher, H. Braunschweig and C. Lambert, *Phys. Chem. Chem. Phys.*, 2015, **17**, 11848.
15 a) B. Wang, X. Chai, W. Zhu, T. Wang and Q. Wu, *Chem. Commun.*, 2014, **50**, 14374; b) J. Yang, M. R. Karver, W. Li, S. Sahu and N. K. Devaraj, *Angew. Chem. Int. Ed.*, 2012, **51**, 5222.
16 J. B. Grimm, B. P. English, J. Chen, J. P. Slaughter, Z. Zhang, A. Revyakin, R. Patel, J. J. Macklin, D. Normanno, R. H. Singer, T. Lionnet and L. D. Lavis, *Nat. Methods*, 2015, **12**, 244.
17 J. E. Hoffmann, T. Plass, I. Nikić, I. V. Aramburu, C. Koehler, H. Gillandt, E. A. Lemke, C. Schultz, *Chem. Eur. J.* 2015, **21**, 12266.
18 a) T. Plass *et al., Angew. Chem. Int. Ed.* 2012, **51**, 4166; b) I. Nikić, T. Plass, O. Schraidt, J. Szymański, J. A. Briggs, C. Schultz and E. A. Lemke, *Angew. Chem. Int. Ed.* 2014, **53**, 2245; c) E. Kozma, I. Nikić, B. R. Varga, I. V. Aramburu, J. H. Kang, O. T. Fackler, E. A. Lemke and P. Kele, *ChemBioChem*, 2016, **17**, 1518; d) K. Lang, L. Davis, J. Torres-Kolbus, C. Chou, A. Deiters and J. W. Chin, *Nat. Chem.* 2012, **4**, 298; e) I. Nikić *et al.*, *Angew. Chem. Int. Ed.*, 2016, **55**, 16172.
19 R. S. Erdmann et al., Angew. Chem. Int. Ed., 2014, 53, 10242.
20 N. Banterle *et al.*, *J. Struct. Biol.*, 2013, **183**, 363.